Correction of self-illumination for pressure and temperature sensitive paints

Oleg Gobyzov[1*], *Artyom* Rabetskiy[2], and *Artur* Bilskiy[1]

[1]Kutateladze Institute of Thermophysics, Siberian Branch of Russian Academy of Sciences, 630090, Novosibirsk, Russia
[2]Sigma-Pro LLC, 630090, Novosibirsk, Russia

Abstract. The present work reports self-illumination correction procedure and results of its experimental testing on a simple model. In the procedure reflectivity value is assessed directly from the set of model images captured at wind-off conditions with different reflecting surfaces covered or removed. The paper covers the theoretical part of the problem and describes exact implementation of a processing sequence, which included image mapping on a 3-D surface, building a mesh of surface elements, evaluation of radiative exchange between elements and calculation of the corrected brightness map.

1 Introduction

Pressure and Temperature sensitive paints (PSP and TSP) [1] are optical techniques for measurement of the spatial distributions of pressure and temperature on surfaces. Both techniques are mostly employed in aerodynamics. They are based on imaging of the luminescence of special layers, applied on the surfaces. Luminescent layers are sensitive to temperature and pressure variations because of the quenching mechanisms, which allows evaluating pressure and temperature distributions on the surfaces from the image brightness through the calibration procedures.

PSP and TSP techniques have different sources of error, related to experimental conditions, equipment characteristics, imaging and data processing. One of such error sources is so-called secondary reflection or self-luminescence. It occurs at concave surfaces, surface joints and internal angles due to the radiative exchange between surfaces. For example, in two-surface configuration, a reflected excitation light and emitted luminescent light propagate from the one surface to another and then, being reflected or absorbed (with subsequent emission) at the second surface, form brightness variations in the image that are not related to the pressure or temperature distribution. An illustration of self-luminescence in configuration with two plane surfaces is shown in fig 1a.

There are several methods for the elimination of this effect. Elimination of the part, related to the excitation light reflections can be performed by the so-called 'wind-off' correction procedure, but it does not solve the problem in general. The effects of self-illumination in PSP and procedures of its correction were studied by Ruyten and Fischer [2], and Le Sant [3]. In order to perform a correction, one must account for the 3D-shape of the surfaces and reflectivity, or, in more general case - bidirectional reflectance distribution function (BRDF) over the surfaces. Correction procedures usually employ a diffusive surface model, but a reflectance value, required for the correction, poses a separate problem.

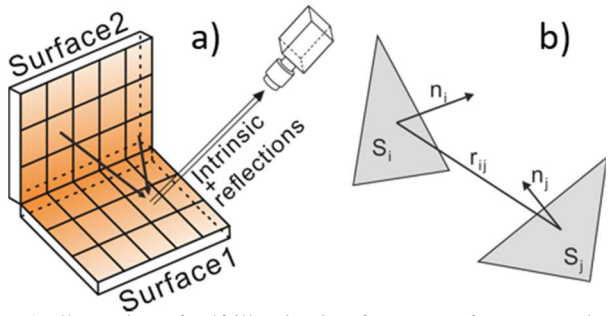

Fig. 1. Illustration of self-illumination for two surfaces (a) and spatial configuration of surface elements (b).

In the present work, a realization of a self-illumination correction procedure is reported and results of its experimental testing are shown. Instead of direct radiometric measurement of the reflectivity, its value is assessed from the set of images captured at wind-off conditions with different reflecting surfaces removed or covered. Other steps of the correction procedure include 2-D brightness field (image) reprojection on the 3-D surface, building a mesh of surface elements, evaluation of radiative exchange between elements and calculation of the corrected brightness map.

2 General description of the problem

To correct PSP/TSP data for self-luminescence several steps of the data processing and preparation should be performed. Particularly, a mapping of the image to the 3-D surface of the model is required, which means that model geometry should be known in advance.

Today methods of surface geometry reconstruction (3D scanning) are very versatile and common in many

* Corresponding author: oleg.a.g.post@gmail.com

applications. A good survey of such methods is provided by Daneshmand et al in [4]. For the PSP/TSP methods it is preferred that the mapping is available with information acquired directly from the luminescence image. This is usually performed using reference points (markers), position of which on a 3D-surface is known [5]. Ideally, every pixel of the image should be bijectively mapped to the 3D-surface.

The self-luminescence correction is based on the idea that the total brightness of each element *i* consists of its own 'intrinsic' luminescence and 'external' incident light from other elements *j*, reflected from element *i*. In a general case of reflecting surface, for each point of the surface, there is a function that connects an angular distribution of the reflected light intensity to the incidence angle of incoming light (so-called spatially varying bidirectional reflectance distribution function, SV-BRDF). In case, if all of the surface points have similar reflection properties, the reflection properties of the whole surface are described by the BRDF that does not account for the position of the point. Calibration for the BRDF is still quite complicated and often a diffusive reflection model, in which luminance is equal for all directions of observation, is employed. In this case, reflection properties of the surface are described by a single reflectivity coefficient *R*. A diffusive model is justified for at least one type of PSP in [2]. Moreover, any model with nonuniform BRDF drastically complicates calculations, which makes diffusive model more suitable in practice. With a diffusive reflection model a total brightness luminance of the element *i* is:

$$I_i = I_{lum,i} + I_{refl,i} = I_{lum,i} + R_i \sum_j^N I_j K_{ij} \tag{1}$$

where R_i is the surface element reflectivity, N is the number of other elements involved in a radiative exchange with element indexed *i*, and K_{ij} is a form factor or 'geometric factor', that takes into account size, position and orientation of the elements. Note, that we still hold the index for the reflectivity, assuming that it's value is a property of a considered element. K_{ij} depends on the position and orientation of elements *i* and *j* and on the surface area of element *i:*

$$K_{ij} = \frac{\left(r_{ij}, n_i\right)\left(r_{ij}, n_j\right)}{\pi \left|r_{ij}\right|^4} dS_i \tag{2}$$

where n_i and n_j are unit normals to the surface elements and r_{ij} is the distance vector between elements (see also figure 1b). Mentioned considerations can be also found, for example, in [2] and [3].

If a 2-D brightness distribution (image) is mapped to the 3-D model surface, all of the values in eq (1) can be evaluated, except for the reflectivity. The reflectivity value, though, should be acquired from separate measurements. In [2] and [3] radiometric measurements were suggested to acquire reflectance value. In the current work, an alternative approach of reflectivity estimation directly from the luminescence images is proposed. A very similar approach was suggested in [6], though in this work a separate unit consisting of two rectangular plates, connected at one side through a regulated joint, was proposed for calibration and the average reflectivity value for the paint was assessed without 3D-mapping of the image.

For the proposed approach, first, an image of the surface, for which a reflectivity value is required, without outer sources of light that may be reflected is taken. After that, another image with one or more external light sources is captured. To avoid errors, both images should be taken at the same conditions, such as temperature, pressure, excitation and ambient light. In this case, the total brightness in the second image can be separated into intrinsic and reflected parts using first image and the reflectivity value can be evaluated. Let us consider the case with two surfaces: first is the surface, for which *R* is evaluated, and the second is the source of external light. In this case *Ri* for each element *i* of the first surface is evaluated as follows:

$$\begin{aligned}
I_{1,i} &= I_{lum,i} + R_i \sum_j^{N1} I_j K_{ij} \\
I_{2,i} &= I_{lum,i} + R_i \left(\sum_j^{N1} I_j K_{ij} + \sum_j^{N2} I_j K_{ij} \right) \\
I_{1,i} - R \sum_j^{N1} I_j K_{ij} &= I_{2,i} - R_i \left(\sum_j^{N1} I_j K_{ij} + \sum_j^{N2} I_j K_{ij} \right) \\
R_i &= \frac{\left(I_{2,i} - I_{1,i}\right)}{\sum_j^{N2} I_j K_{ij}}
\end{aligned} \tag{3}$$

R_i can be used as a spatially varying reflectivity function if reflectivity exhibits noticeable variations over the surface. Alternatively, R_i can be averaged over the surface to acquire a single reflectivity coefficient. The rest of the correction procedure implies solving the equation (1) for each element of emitting/reflecting surfaces that take part in the radiative exchange. In the next sections, a setup for experimental testing of the correction procedure and realization of the processing scheme are considered.

3 Experimental setup

To test the procedure a simple model of 3 small rectangular plates assembled into the 90° internal angle with 3 walls was manufactured (see figure 2). A PtTFPP pressure-sensitive paint was applied on the surfaces of the plates.

For the mapping of the image brightness onto the 3D-model a set of 9 evenly spread markers was manually applied on each of the angle sides. A number of markers was excessive, but additional markers could improve the precision of mapping and could be used in verification of the mapping procedure.

A high-power LED with a maximum emission wavelength at 390 nm and emission spectra half-width at half maximum of about 20 nm was used as the excitation light source. LED was operated in pulse mode with pulse length of about 100 μs and was synchronized with a camera. Images were captured with a scientific-grade CCD-camera with 1 Mpix image resolution in 14-bit mode and saved as 16-bit images. The image resolution

was 70 μm per pixel. The camera lens was supplied with a band-pass filter to suppress excitation light and stray background light. To reduce random error in image brightness for each configuration statistics of 100 images was captured and series-averaged images were used for further processing.

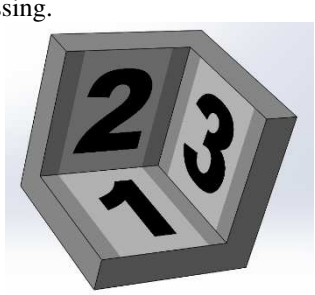

Fig. 2. Test model with 3 luminescent walls. Numbering is according to the one employed in the paper.

To exclude luminescence of separate surfaces from images they were covered with matte black sheets. The model images were captured in three configurations: with surfaces 2 and 3 covered, so that only intrinsic luminescence of surface 1 was visible, with surface 3 covered and with all three surfaces visible. An example of images is shown in figure 3.

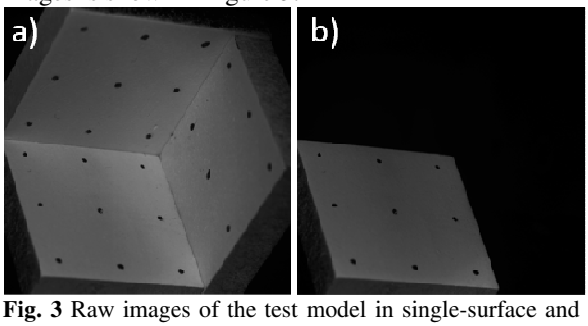

Fig. 3 Raw images of the test model in single-surface and 3-surfaces configuration.

4 Processing sequence

4.1 Data preparation

All of the processing, except for the initial 3D surface modeling, was performed using Python 3.5 and open-source libraries for this programming language. An initial 3D surface model of the plates assembly was created in CAD software and stored in the STL format, which describes surface as a set of adjacent triangles (unstructured triangular mesh) and unit normals to the triangles. As it was mentioned before, ideally, a mesh resolution should be enough to provide mapping of each pixel to a separate triangle vertex. To fulfill this requirement more than $3 \cdot 10^5$ vertices for one plate and about $2 \cdot 10^{11}$ rays in ray tracing must be evaluated. To avoid heavy calculations a 3D-surface mesh resolution was reduced to 0.5 mm, which was still much smaller than the characteristic size of brightness variations. Note, that STL format was used merely as a tool for mesh building and navigating over vertices. Brightness values were projected onto the vertices, and for the future evaluation a surface area *dS*, equal to the triangle area, and a unit normal, calculated form the normals of adjacent triangles, were assigned to each vertex.

The next step was a search of markers position in the image and calculation of camera model parameters for image mapping. A markers search was performed using the 'SimpleBlobDetector' method from OpenCV library.

The projection parameters were acquired from the camera transform equations, that connect 3-D spatial coordinates of an object and the corresponding 2-D spatial coordinates in an image [5]. Internal camera orientation parameters were measured separately using a calibration target to achieve better parameters fitting. Parameters of projection were fitted using the Levenberg-Marquardt algorithm. In fact, solving a series of equations requires 6 points with known coordinates in 3-D space and in the image, thus, larger number of markers served mainly for random error reduction.

The final 3D model contained about $2 \cdot 10^5$ vertices (about $9 \cdot 10^4$ visible), for each of those 3 sets of data were stored: a brightness value, a reference pixel coordinates, and visibility information, indicating if the vertex is seen in the image.

4.2. Self-luminescence correction

A self-luminescence correction procedure was based on the ray-tracing method. To perform required calculations for each vertex on the considered surface a set of rays, connecting the vertex with all other vertices in the model was built. In general, each ray should be checked for occlusion, i.e. it should be checked whether there are any obstacles that block the light path. Although the tested model does not require such check due to relatively simple configuration, it was still implemented in a processing sequence. The occlusion check was based on the BVH algorithm [7] with an STL model as an input data.

The reflectivity of the surface was estimated as described in the 'general description' section. For this purpose, images with only one visible surface and with two visible surfaces were used. The first step for reflectivity calculation is the evaluation of form factor in two-surface system for the elements of the surface 1, for which the correction was to be performed.

A diffusive emission model, in which the light, emitted from the surface is evenly distributed in a half-space in front of the surface element, was employed. An assumption that all the light from the vertex is emitted directly from the vertex point was also used, although each vertex has an assigned surface area value. The assumption is valid if the distance between emitting and reflecting elements is much larger than the size of any of the elements.

With these assumptions, a form factor for each element can be evaluated from the eq. (2). Knowing the intrinsic luminescence brightness for each element $I_{lum\ 1,i}$ of the surface 1 (from the images with only this surface visible), brightness of each element $I_{2,j}$ of the surface 2, and all required form-factors, it is possible to evaluate $R_{i,1}$ of each element of the surface 1 and average R for the whole surface.

Finally, after the evaluation of *R*, a self-luminescence correction can be performed. To test the validity of the correction, an image of the model with three luminescent surfaces was used. In this case, the surface 1 is illuminated by a light emitted from the surfaces 2 and 3. Using the same approach, the image was mapped to the 3-D model and the amount of light incident from surfaces 2 and 3 onto each of the elements of the surface 1 was calculated and then subtracted from the total brightness of those elements. Brightness distributions in corrected and initial brightness maps on the 3-D surface are shown in figure 4. Acquired distributions show, that corrected brightness qualitatively match the luminescence of single surface, but the correction with distributed reflectivity produce more noise in the data.

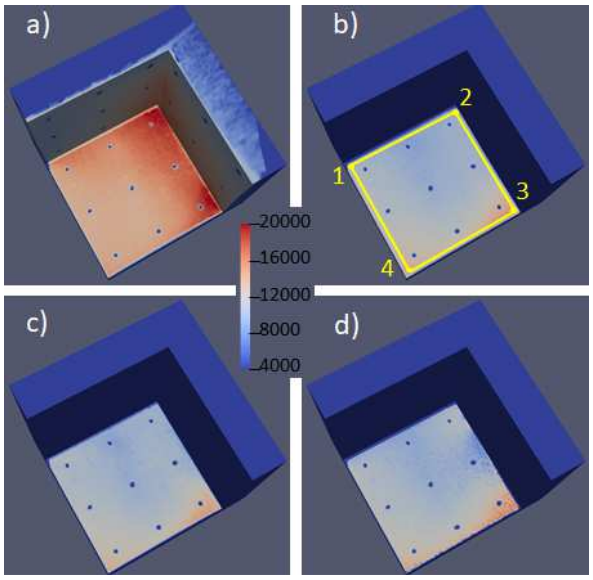

Fig. 4. Brightness maps on a 3D-model. a) 3-surface configuration, not corrected, b) single-surface configuration, c) 3-surface configuration, corrected with average *R*, d) 3-surface configuration, corrected with distributed *Ri*.

The luminescence profiles for corrected and uncorrected images with three surfaces and corrected luminescence versus luminescence with only one surface visible are shown in figure 5. The profiles were built along the closed line, shown in fig. 4b. Each section of the line was parallel to the border of the plate and was placed at a distance of 2.5 mm from the border. The normalized difference between corrected brightness and single surface brightness is presented in figure 6.

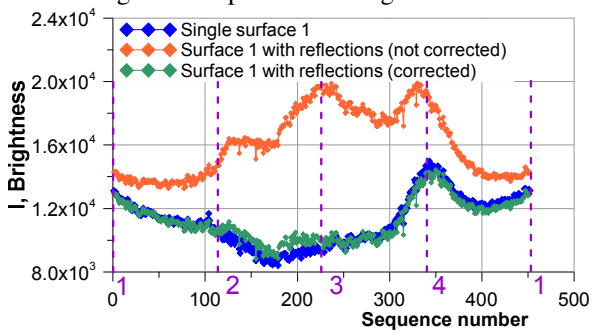

Fig. 5. Brightness profiles in corrected and initial brightness maps on the 3-D model.

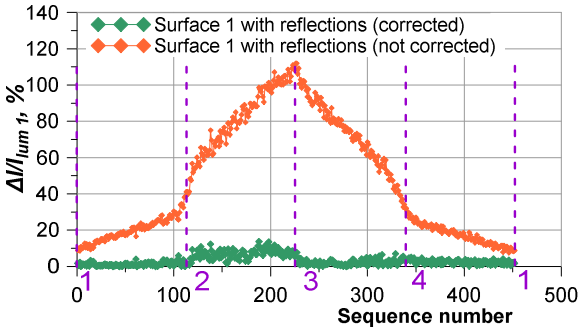

Fig. 6. Relative error before and after correction.

These profiles show, that self-luminescence was successfully corrected over the whole surface. Small discrepancy (within 10% of single plate image brightness) can be seen in the vicinity of the joint of three surfaces. There can be several sources of this residual difference: a misalignment in projection and back-projection of the brightness map, effect of the reflections of higher orders, and non-validity of the element infinitesimality assumption near the wall. More precise mapping and an increase in 3D-model resolution, as well as reflectivity calculation from several model configurations could further improve the result.

5 Conclusion

A variation of the method for the correction of self-luminescence in PSP/TSP experiment has been presented. The method was experimentally tested and allowed to reduce the error, related to the self-luminescence from more than 100% to 10%. The proposed approach for reflectivity estimation can be applied directly to the model in situ. It should be noted, that at least in current implementation the processing sequence is quite computationally heavy, so for more complex models and higher spatial resolution it requires further optimization in order to provide reasonable processing time for experimental data.

Acknowledgments: The work was carried out within the state assignment of Ministry of Science and Higher Education of the Russian Federation.

REFERENCES

1. T. Liu, J.P. Sullivan, *Pressure and temperature sensitive paints* (Springer-Verlag, 2005)
2. W. M. Ruyten, C. Fisher, AIAA J., **39 (8)**, 1587 (2001)
3. Y. Le Sant, ICIASF ’2001 Record, 19th International Congress on Instrumentation in Aerospace Simulation Facilities’, 5.2, (2001)
4. M. Daneshmand, A. Helmi, E. Avots, F. Noroozi, F. Alisinanoglu, H. Arslan, J. Gorbova, R. Haamer, C. Ozcinar, G. Anbarjafari, arXiv:1801.08863 (2018)
5. A.W. Burner, T. Liu, J. of aircraft, **38 (4)**, 745 (2001)
6. W. M. Ruyten, Rev. Sci. Instr., 68, 3079 (1997)
7. J. Goldsmith, J. Salmon, IEEE Computer Graphics and Applications, 7 (5), 14 (1987)